Zagazig J. Pharm. Sci. Dec, 2023
Vol. 32, Issue 2, pp. 64-85

ISSN 1110-5089
ISSN (on-line) 2356_9786

Optimizing the transdermal delivery of Granisetron via chitosan-coated liposomal vesicles using 2^4 full factorial design

El-Shanawany, Maged A.[*,1] Hasan Azza A[1] , Abu-Zaid Samir S[1]. , Sabry Shereen A[1] ,

[1]Department of Pharmaceutics, Faculty of Pharmacy, Zagazig University

*magedelshanawany@gmail.com , 01095464764

Received:23 Aug 2023 /Accepted: 16 Oct 2023
DOI: 10.21608/ZJPS.2023.231377.1053

ABSTRACT

The present study focused on developing and evaluating chitosan-coated liposomal vesicles as a transdermal drug delivery system for granisetron hydrochloride, a potent antiemetic drug used in chemotherapy-induced nausea and vomiting Minitab 21.4 software was used to optimize granisetron delivery systems through a 4-factor, 2-level full factorial design. This investigation focused on key formulation factors: preparation method, drug/lipid fraction, lecithin type, chitosan coating, and their impact on critical responses. This approach helped to identify factors of high significance in the model equation, enhancing the understanding of granisetron formulation optimization.. Physicochemical properties, drug release profile, release kinetics, and ex vivo skin permeation studies were conducted to assess the liposomal formulations. The optimization process aimed to achieve specific targets, including a particle size of approximately 120 nm and a zeta potential of +35 Ve. The chosen optimal formulation exhibited favorable values, with an entrapment efficiency of 47.29% ± 2.23 , particle size of 137.25 nm± 5.72 , zeta potential of 17.14 Ve ± 1.71 , and dissolution efficiency of 86.82%± 7.68 . Further, The optimized liposomal gel formulation demonstrated a 25% increase in flux (27.73 $\mu g.cm^{-2}.hr^{-1}$) compared to the raw drug-loaded gel (22.03 $\mu g.cm^{-2}.hr^{-1}$) for the permeation of granisetron through the skin. These findings underscored the superior drug delivery capabilities of the liposomal systems and their potential for improving therapeutic outcomes in the targeted application. The results indicated that the liposomal-loaded formulations had the potential to enhance the transdermal delivery of granisetron compared to conventional gel formulations.

Keywords : Granisetron; liposomes; transdermal delivery; phosopholipid; chitosan; particle size; zeta potential; dissolution efficiency.

INTRODUCTION

Chemotherapy-induced nausea and vomiting are commonly distressing side effects experienced by cancer patients undergoing treatment (1,2). To alleviate or minimize these adverse effects, serotonin receptor antagonists targeting the 5-hydroxytryptamine (5HT-3) subtype-3 have been widely employed. 5HT-3 antagonists such as tropisetron, and granisetron are frequently administered either through injections or orally on a daily basis (3).

Granisetron is a potent and selective 5HT-3 receptor antagonist known for its antiemetic properties. When administered orally, it is rapidly absorbed from the gastrointestinal tract, with peak serum concentration reached within approximately 2 hours (4). One limitation of oral administration

ISSN 1110-5089
ISSN (on-line) 2356_9786

is that granisetron undergoes first-pass metabolism, which can result in reduced bioavailability (60%) (5). Therefore, there is a need to develop alternative delivery methods, such as a transdermal formulation, to improve drug bioavailability and enhance patient compliance (6).

In 1998, Touitou and colleagues revolutionized the field of transdermal drug delivery by introducing vesicles as a breakthrough approach. These vesicles, or liposomes, are small membrane-enclosed sacs composed of a phospholipid bilayer that can encapsulate hydrophilic and lipophilic drugs, protecting them from degradation and improving their permeability (7). They are widely used as drug delivery systems due to their biocompatibility, biodegradability, and ability to encapsulate both hydrophilic and hydrophobic drugs (8). Liposomes were proved to be a promising means of storing and transporting substances within living cells. This discovery paved the way for more effective and efficient transdermal drug administration. The transdermal delivery of antiemetic drugs presents an intriguing approach that holds promise for effectively managing chemotherapy-induced nausea and vomiting (9). This method involves delivering the antiemetic drug through the skin, allowing systemic absorption. Transdermal drug delivery offers numerous advantages, particularly for patients experiencing specific symptoms. By utilizing this method, the antiemetic drug can bypass the gastrointestinal system altogether, entering the bloodstream directly. As a result, it provides more reliable and controlled drug levels, potentially leading to enhanced efficacy and improved patient compliance compared to traditional oral or injectable routes (10,11). Moreover, transdermal delivery has the potential to reduce the frequency of drug administration and alleviate the burden of daily dosing for patients.

Quite a few studies have investigated using vesicular systems for transdermal delivery of granisetron. For example, one study reported the development of a proniosomal gel containing granisetron for transdermal delivery (12). The proniosomes were prepared using a combination of Span 60 and cholesterol, which significantly improved the bioavailability of granisetron compared to a conventional gel. The results revealed that the cumulative release and flux of the proniosomal gel were approximately twice as high as those of the drug solution with the same drug concentration. This study effectively demonstrated the potential of proniosomal transdermal patches containing granisetron HCl to efficiently manage chemotherapy-induced nausea and vomiting. Another study investigated the use of transferosomes for transdermal delivery of granisetron (13). The elastic liposomes were prepared using a combination of phospholipids, cholesterol, and an edge activator and were found to provide sustained drug release over 24 hours, with improved bioavailability compared to a conventional gel (7,8,14). Liposomes can potentially increase the bioavailability of granisetron and improve its pharmacokinetics and pharmacodynamics. However, to date, limited studies have investigated the use of liposomes for granisetron delivery. These findings highlight the superior drug delivery capabilities of the vesicular drug delivery systems, emphasizing its potential for enhanced therapeutic outcomes in this specific application.

Therefore, the present study aims to develop and evaluate liposomes as a drug delivery system for granisetron. The liposomes will be prepared using different phospholipids and surface coating with chitosan, and their physicochemical properties, drug release profile, drug release kinetics and ex-vivo skin permeation studies will be investigated.

1. Materials

Zagazig J. Pharm. Sci. Dec, 2023 ISSN 1110-5089
Vol. 32, Issue 2, pp. 64-85 ISSN (on-line) 2356_9786

Granisetron was supplied by Amoun Pharmaceutical Industries Co. Egypt. Cholesterol, egg and soya lecithin were gifted from Egyptian International Pharmaceutical Industries (EIPICO) Co. Egypt. Low molecular weight chitosan was purchased from Sigma Aldrich. Tween 80, hydroxypropyl methylcellulose grade E4 (HPMC E4), potassium dihydrogen orthophosphate and disodium hydrogen orthophosphate were supplied by EL-Nasr Pharmaceuticals Chemicals Co., Egypt. Chloroform and Sodium carboxymethyl cellulose (Na CMC) were purchased from Adent Ltd., India. Diethyl ether was obtained from Sisco Research Laboratories Pvt, Mumbai, India. All other chemicals were of analytical grade.

2. Methods

2.1. Design of the experiment and statistical analysis

Experimental design is an established approach used to study the relationship and interaction between independent variables (factors) and dependent variables (responses). In this particular study, a commonly used software (Minitab 21.4) was utilized for experimental design, mathematical treatments, and statistical data analysis (15) A 4-factor, 2-level (2^4) full factorial design was employed. The purpose of the design was to optimize selected formulation factors and assess the main and interaction effects on the responses of interest. The factors selected for this study were the preparation method (A), drug/lipid fraction (B), lecithin type (C), and chitosan coating (D). The responses being studied were the entrapment efficiency percentage (EE%) of granisetron (Y_1), particle size (Y_2), zeta potential (Y_3), and dissolution efficiency percentage (DE%) of granisetron. Table 1 displays the two levels of the tested factors and the desired goals for the responses. The design software suggested random sixteen runs, which were listed in Table 2. After obtaining the response data, the factorial analysis was adopted using Minitab software, which was used to fit the data values and analyze the results. The Akaike information criterion corrected was applied to include the factors with high significance in the model equation.

Table 1: Selected independent factors and goal of the dependent responses for the optimal granisetron-loaded liposomal formulation.

Independent factors	Unit	Type	Actual coded levels	
			Low (-1)	High (+1)
Preparation method (A)	-	Categorical	TFH	EI
Drug/Lipid fraction (B)	-	Numerical	0.5	1
Lecithin type (C)	-	Categorical	Egg	Soya
Chitosan percentage (D)	%	Numerical	0	0.25
Dependent factors			**Goal**	
Entrapment efficiency (Y_1)	%		Maximize	
Particle size (Y_2)	nm		120	
Zeta potential (Y_3)	-Ve		+35	
Dissolution efficiency (Y_4)	%		Maximize	

TFH: Thin Film Hydration, EI: Ether Injection

3.2. Preparation of liposome

3.2.1Thin film hydration method

The following thin film hydration procedure was employed for the preparation of liposomes containing granisetron (16,17). Initially, a mixture of lecithin and cholesterol was solubilized in 10 ml chloroform and then dried at 37±1 °C via a rotary evaporator for 2 hours under vacuum. The ratio of lecithin to cholesterol was maintained at 2:1, while the granisetron/total lipid ratio was altered during the experiment, ranging from 1:2 to 1:1. The dried lipid films were hydrated with 10 ml phosphate buffer (pH = 7.4) preheated at 70 °C and containing 2% tween 80 and either 6 or 12% granisetron. The hydration process was performed at 25±1 °C for 2 hours till the liposomal dispersion was attained.

3.2.2.Ether injection method

The ether injection method was previously reported for the efficient production of liposomes (18,19). To prepare the liposomal

Zagazig J. Pharm. Sci. Dec, 2023
Vol. 32, Issue 2, pp. 64-85

ISSN 1110-5089
ISSN (on-line) 2356_9786

dispersion for granisetron, a mixture of lecithin and cholesterol was dissolved in 5 ml diethyl ether. In a beaker, granisetron was continuously stirred with phosphate buffer (10 ml, pH 7.4) containing 2% tween 80 under magnetic stirring and maintained at a temperature of 55-60°C. The solution containing lipids was slowly injected into the beaker with the help of a syringe to disperse the solution in phosphate buffer. The beaker was continuously stirred on a magnetic stirrer at 40 °C until the ether was completely evaporated, forming a semitransparent liposomal dispersion.

Table 2. Composition and characterization parameters of granisetron-loaded liposomal formulations

Code/ Symbol	A Preparation method	B Drug/Lipid fraction	C Lecithin type	D Chitosan (%)	Y1 Entrapment efficiency (%)	Y2 Particle size nm	Y3 Zeta potential mV	Y4 Dissolution efficiency (%)
F1	EI	0.5	Soya	0.00	52.40±1.32	86.66±2.70	-16.3±1.47	79.95±2.54
F2	TFH	1.0	Egg	0.00	59.20±1.75	175.40±15.15	-16.7±0.52	84.02±2.69
F3	TFH	1.0	Egg	0.25	46.40±1.22	606.40±22.06	+41.0±0.75	89.44±3.12
F4	TFH	0.5	Egg	0.25	48.08±2.43	670.90±50.89	+45.0±0.20	89.78±3.65
F5	TFH	0.5	Soya	0.00	58.10±1.19	169.20±5.88	-17.6±0.31	79.78±2.53
F6	EI	1.0	Soya	0.25	47.30±3.66	159.20±5.65	+30.9±0.50	88.80±3.42
F7	TFH	1.0	Soya	0.00	56.20±2.69	169.40±14.64	-17.2±0.68	85.40±3.95
F8	EI	1.0	Egg	0.25	46.00±1.98	341.70±4.10	+40.5±1.05	89.60±4.27
F9	TFH	0.5	Egg	0.00	58.40±2.87	324.40±29.18	-31.1±1.54	79.37±3.43
F10	TFH	0.5	Soya	0.25	47.40±3.24	496.20±25.44	+38.3±1.85	89.05±3.22
F11	EI	0.5	Egg	0.25	45.00±2.56	325.00±12.45	+46.8±1.05	89.50±2.36
F12	EI	1.0	Egg	0.00	54.00±2.12	65.02±1.02	-16.1±0.80	84.20±2.48
F13	EI	1.0	Soya	0.00	52.40±2.03	84.86±2.53	-16.7±1.23	83.44±2.55
F14	TFH	1.0	Soya	0.25	46.50±1.85	630.50±27.98	+38.2±1.03	90.47±3.28
F15	EI	0.5	Egg	0.00	57.10±2.56	338.10±5.55	-31.0±0.80	80.29±2.43
F16	EI	0.5	Soya	0.25	43.90±1.47	160.70±13.78	+46.9±0.81	90.69±2.13

3.2.3. Chitosan coating procedure

Chitosan was previously reported to produce an efficient coating of the liposomal vesicles (20,21). Chitosan solution was prepared at a concentration of 0.5% (w/v) by dissolving in water containing acetic acid 0.35% (v/v). The suspended liposome vesicles were then dropped into an equal volume of the chitosan solution while stirring. The mixture was stirred for 1 hour and then stored overnight under cooling conditions 4 °C. The resulting coated liposomes were collected by centrifugation at 15,000 rpm for 20 min under cooling conditions. The suspension was reconstituted again for further testing.

3.3. Characterization of the prepared liposomes

3.3.1 Drug entrapment efficiency percentage:

The entrapment efficiency of granisetron-loaded liposomal dispersion was determined by the dialysis method (22). Cellophane membranes were hydrated in phosphate buffer pH 7.4, and the formulations were transferred into dialysis bags formed of cellophane membrane (MWCO: 12–14 kDa) (Fisher Sci.Co., USA) placed in glass bottles with the same buffer as the receptor medium. Shaking in a Kotterman shaker water bath (Julabo SW–20C, Germany) at 25±1 °C and 100 rpm, the receptor media were filtered using 0.22 µM nylon filter and analyzed using a spectrophotometer at λ_{max} 297 nm to quantify the free granisetron. A fresh receptor medium was used until no granisetron was detected. Entrapment efficiency was calculated as the ratio of the entrapped granisetron to the initial total drug amount as presented in the following equation:

$$Drug\ entrapment\ efficiency = \frac{Experimental\ granisetron\ content}{Theoretical\ granisetron\ content}\ x\ 100$$

3.3.2. Particle size and zeta potential

The size distribution of the granisetron-loaded liposomal dispersion was analyzed using dynamic light scattering (DLS) following the procedure described by Shaker et al. 2017 (23). The liposomal vesicles were suspended in double-distilled water, vortexed, and sonicated for 2 minutes to ensure homogeneity. The average hydrodynamic diameter of the liposomal vesicles was determined using a Zetasizer Nano ZS instrument (Malvern Instruments, UK) (24).

3.3.3. In vitro drug release

The dissolution behavior of the granisetron-loaded liposomal formulations was evaluated *in vitro* using the dialysis bag method, as previously discussed. Under sink condition, 6 mg of pure granisetron and equivalent amounts of liposomal dispersion were added to 50 ml of phosphate buffer (0.05 M, pH 7.4) and stirred at

ISSN 1110-5089
ISSN (on-line) 2356_9786

100 rpm at 37 ± 0.5 °C. Aliquots of 1 mL were withdrawn at predetermined time intervals (0.5, 1, 2, 3, 4, and 6 hr), and filtered before measuring the drug content spectrophotometrically at λ_{max} of 297 nm. The dissolution test was conducted in triplicate, and the results were expressed as mean values ± standard deviation.

3.4. Characterization of the optimized formulation

3.4.1. Particle size and zeta potential

The particle size and zeta potential of the optimized formulation was carried out as described earlier.

3.4.2. Transmission electron microscopy

To visualize the liposomal vesicles, a small amount of the liposomal dispersion was placed on carbon grids and allowed to dry at room temperature. The dried sample was stained with a 1% aqueous phosphotungstic acid solution, and there were imaged using Thermo Scientific Talos™ F200i.

3.4.3. Differential scanning calorimetry

The compatibility and entrapment of granisetron and the liposomal excipients at a physicochemical level were evaluated using a differential scanning calorimeter Perkin Elmer DSC 4000. The optimized formulation was lyophilized prior to DSC testing. The samples were subjected to heat in enclosed aluminum pans at a constant heat flow rate of 10 ^{o}C/min, while being purged with nitrogen gas at a flow rate of 30 mL/min.

3.4.4. Attenuated total reflectance-Fourier transform infrared (ATR-FTIR)

To investigate the nature of interactions between the granisetron and the liposomal components at the solid-state level for the lyophilized sample. ATR-FTIR spectroscopy was performed. The spectra were acquired using a Thermo Scientific Nicolet™ IS50 FTIR spectrometer, covering a frequency range of 500-4000 cm^{-1}.

3.5. Preparation of the liposome-loaded hydrogel:

The hydrogel was prepared by suspending the liposome vesicles into two different hydrogel bases (Na CMC 2% and HPMC E4 3%, w/v). The gel base was dissolved under gentle stirring and stepwise addition of the gel powder prior to the addition of liposomes.

3.6. Characterization of the liposomal hydrogels:

The drug-loaded liposome hydrogel was subsequently subjected to characterization tests as follow :

3.6.1. pH measurements:

Before the measurement, the pH meter underwent calibration to ensure accuracy. Subsequently, the electrode was immersed in the prepared hydrogel until a stable reading was obtained. Triplicate measurements were recorded for each sample, and the results were presented as mean values ± S.D. (25,26).

3.6.2. Drug content:

Each gel sample weighing 0.25 gm was dissolved in 10 ml of methanol and vortexed for 5 minutes to ensure complete drug extraction. The resulting solution was filtered using a 0.45 µm nylon syringe filter, and the drug content in the filtrate was analyzed spectrophotometrically at λ_{max} 297 nm against a blank of methanol. The experiment was repeated three times, and the results were reported as mean values ± S.D.

3.6.3. Viscosity measurements:

The viscosity of each base was determined using a rotating viscometer (Visco Star-R) at 10 rpm with spindle number 6 under ambient temperature conditions. The viscosity measurements were conducted in triplicate, and the results were reported in Centipoise units.

Zagazig J. Pharm. Sci. Dec, 2023
Vol. 32, Issue 2, pp. 64-85
ISSN 1110-5089
ISSN (on-line) 2356_9786

3.6.4. In vitro drug release study:

The release of granisetron from the liposomal gel formulations was performed using cellophane membrane dialysis tubing. Every 2 grams of the hydrogel formulations containing 6 mg of granisetron were transferred to the dialysis bags. The bags were then sealed and suspended in sealed bottles containing the receptor medium (50 ml of phosphate buffer (pH 7.4)). The release media were kept at 37 ± 1 ^{o}C and stirred at 100 rpm in a thermostatically controlled shaking water bath. Aliquots of 1 ml were collected at fixed time intervals (0.5, 1, 2, 3, 4, and 6 hr) and filtered using 0.45 µm syringe filters. Fresh medium was added to substitute the withdrawn amounts and to maintain the constant volumes. The granisetron content in the withdrawn samples was measured at λ_{max} 297 nm, and each measurement was carried out in triplicate and expressed as mean values ± S.D.

3.6.5. Ex-vivo skin permeation study:

3.6.5.1. Preparation of rabbit skin:

The dorsal layer of the ear skin was excised from the sacrificed adult albino rabbits using scalpel, and fur from this area was trimmed by a clipper to avoid gel adsorption to the fur (27). The intact skin was cleaned with distilled water and stored in the receptor medium (phosphate buffer pH 7.4 and sodium azide as a preservative) overnight in the refrigerator (28).

The liposomal gel formulations (G3), which showed a desirable *in vitro* granisetron release, was subjected to further permeation studies. The result was compared to the formulation (G1), which contains pure granisetron. After pretreatment, the skin sections were adjusted to fit a permeation area of 5.3 cm^2 of fabricated diffusion cells where the subcutaneous layer faced the gel. The liposomal hydrogels were placed in the donor compartment, and cells were inserted in the plastic cap hole covering the beaker. The tube containing the donor compartment was then sealed with aluminium, whereas 50 ml of phosphate buffer with a pH of 7.4 and sodium azide was added as the receptor medium**.** Cells' temperatures were held at 37 ± 1 ^{o}C and continuously stirred at 100 rpm in a thermostatically controlled shaking water bath. Samples were taken at intervals of 1, 2, 3, 4, 8, and 24 hr. Drug content in each sample was measured following UV-HPLC analytical procedures mentioned below. The cumulative granisetron permeation through the rabbit skin (g/cm^2) for both formulations were presented as a function of time (t).

3.6.5.2. Chromatographic conditions:

Granisetron content measurements were conducted following a previously established HPLC analytical protocol as outlined by Bukka et al. in 2021, with minor adjustments (29). The HPLC analysis employed a Waters™ 2690 Alliance system (Milford, MA, USA) equipped with a Waters™ 996 photodiode array detector. The separation of granisetron utilized a Kromasil C18 (5µm, 4.6 x 150mm) analytical column under ambient conditions. An isocratic approach was adopted using a mobile phase composed of a mixture of 20% acetonitrile and 80% (v/v) of 0.25 mM potassium dihydrogen orthophosphate solution, with pH adjusted to 3.0 using a 1% orthophosphoric acid solution. Prior to use, the mobile phase was filtered through a 0.45 µm Millipore membrane and degassed using ultrasonication. The mobile phase was run at a flow rate of 2 ml/min. The sample was filtered through a 0.22 µm syringe filter, and 100 µl was injected for analysis. Detection of elution absorbance occurred at 218 nm. The entire analysis was conducted at room temperature.

4. Results and discussion

4.1. The effect of formulation variables on EE%

Table 2 presents the EE% of the prepared formulations, with values ranging from 43.90 ± 1.21% (F16) to 59.20 ± 1.28% (F1). Meanwhile,

Zagazig J. Pharm. Sci. Dec, 2023
Vol. 32, Issue 2, pp. 64-85
ISSN 1110-5089
ISSN (on-line) 2356_9786

Table 3 demonstrates the model's significance, as indicated by the model F-values of 74.79, along with a coefficient of determination (R^2) of 0.92, indicating a well-fitted model. The experimented results showed in Table 5 a good fit with the predicted results, as seen in the residuals versus run plot (Figure 1c). The model was based on two linear terms, after the forward selection of terms based on AICc minimization criteria. The half-normal plot and Pareto chart show the significant effects that are selected in the proposed model (Figures 1a and b). The AICc reached its minimum value at 69.34 following eight steps of selection. The model was presented as EE%= 56 - 1.374 A - 38.31 D. Figure 1d graphically represents the single factor effect on the dependent response, which is explained as follows:

4.1.1. The effect of the liposome preparation methods

Based on the results in Table 5, it can be concluded that both the preparation methods, TFH and EI, significantly affect the entrapment of granisetron within liposomal vesicles (F-value = 11.37, P-value = 0.005). Specifically, there was an observed increase in the entrapment efficiency of granisetron when the liposomal formulations were prepared using the TFH method. The EE% of the uncoated liposomes consisting of a 1:1 drug to lipid ratio with egg lecithin, prepared via the EI method (F12), was found to be 54.00 ± 2.12%. In contrast, the formulation containing the same composition was produced through the TFI method (F2) exhibited an EE% of 59.20 ± 1.75%.

4.1.2. The effect of drug/lipid ratio and Lecithin type:

The entrapment efficiency was significantly increased ($p < 0.05$) in all formulations prepared with egg lecithin compared to soy Lecithin formulations. It can also be depicted that when drug/lipid fraction shifted from 1:1 to 1:2, an increase in EE% was seen with all prepared formulations ($p < 0.05$). This might be attributed to the effect of higher cholesterol content, where the bilayer hydrophobicity and stability increase and permeability decreases (12). Moreover, the lecithin type did not exert any significant effect on granisetron entrapment into liposomal vesicles ($p < 0.05$).

4.1.3. The effect of chitosan coating

From the ANOVA statistical assessment, results showed that among the effects of all single factors, only chitosan (D) showed a statistically significant negative effect on entrapment efficiency, with p-values of < 0.0001. It was evident that adding chitosan (0.25%, w/v) led to a decrease in EE% from 54.00 ± 2.12 % to 46.00 ± 1.98% for F12 and F8, respectively. This could be ascribed to the competition between chitosan and the granisetron for binding to the phospholipid. Chitosan carries positive charges and its affinity for the phospholipid surface results in limited available binding sites. These results aligned with the previously reported effect of chitosan on the entrapment of leuprolide (21).

4.1.4. Two-way interactions:

Based on the analysis, the results indicate that none of the interaction terms included in the model showed a significant effect on the EE%. This is further supported by the data depicted in Figure 1e. Additionally, the decision to exclude the Two-way interaction terms from the model was based on their low contribution percentages.

Table 3. ANOVA analysis of the dependent responses

Responses	SS	Adj. MS	F-value	P-value	R^2	Adj. R^2	Pred. R^2	PRESS	AICc
EE%	397.11	198.555	74.79	<0.0001	0.920	0.907	0.878	52.2805	69.34
Particle size	642450	107075	65.38	<0.0001	0.977	0.962	0.929	46582.4	191.19
Zeta potential	14884.0	14884.0	386.84	<0.0001	0.965	0.962	0.954	703.553	109.67
DE%	270.818	90.273	203.24	<0.0001	0.980	0.975	0.965	9.47542	43.82

SS: sum of squares, MS: mean sum of squares, R^2: determination coefficient, Adj. R^2: adjusted determination coefficient, Pred. R^2: predicted determination coefficient, AICc: The corrected Akaike

Zagazig J. Pharm. Sci. Dec, 2023
Vol. 32, Issue 2, pp. 64-85

ISSN 1110-5089
ISSN (on-line) 2356_9786

information criterion, PRESS: predicted residual sum of the square.

Table 4: Residuals of actual and predicted average values of Y1, Y2, Y3, Y4 responses for granisetron-loaded liposomal formulations.

	EE% (Y_1)			Particle size (Y_2)			Zeta Potential (Y_3)			DE% (Y_4)		
Code	Actual Value	Predicted Value	Residual	Actual Value	Predicted Value	Residual	Actual Value	Predicted Value	Residual	Actual Value	Predicted Value	Residual
F1	52.400	54.626	-2.226	86.7	46.9	39.7	-16.30	-20.19	3.89	79.950	79.847	0.103
F2	59.200	57.374	1.826	175.6	181.5	-5.9	-16.70	-20.49	3.79	84.020	84.265	-0.245
F3	46.400	47.796	-1.396	606.6	572.9	33.7	41.90	40.51	1.39	89.440	89.578	-0.138
F4	48.000	47.796	0.204	670.9	690.3	-19.4	45.00	40.51	4.49	89.790	89.758	0.032
F5	58.100	57.374	0.726	169.2	162.5	6.7	-17.80	-20.49	2.69	79.780	79.847	-0.067
F6	47.300	45.049	2.251	159.2	182.7	-23.5	35.90	40.51	-4.61	88.800	89.578	-0.778
F7	56.200	57.374	-1.174	169.4	195.7	-26.3	-17.20	-20.49	3.29	85.400	84.265	1.135
F8	46.000	45.049	0.951	141.7	168.5	-26.8	40.50	40.51	-0.01	89.600	89.578	0.022
F9	58.600	57.374	1.226	324.4	298.9	25.5	-31.10	-20.49	-10.61	79.370	79.847	-0.477
F10	47.600	47.796	-0.196	496.2	553.9	-57.7	34.10	40.51	-6.41	89.050	89.758	-0.708
F11	45.600	45.049	0.551	325.0	285.9	39.1	46.60	40.51	6.09	89.500	89.758	-0.258
F12	54.000	54.626	-0.626	65.0	66.0	-1.0	-16.10	-20.49	4.39	84.200	84.265	-0.065
F13	52.400	54.626	-2.226	84.7	80.2	4.5	-16.70	-20.49	3.79	83.440	84.265	-0.825
F14	46.500	47.796	-1.296	630.5	587.1	43.4	38.20	40.51	-2.31	90.470	89.578	0.892
F15	57.100	54.626	2.474	136.1	183.3	-47.2	-31.00	-20.49	-10.51	80.290	79.847	0.443
F16	43.900	45.049	-1.149	160.7	149.5	11.2	46.90	40.51	6.39	90.590	89.758	0.832

Table 5: Results of ANOVA statistical analysis of EE% (Y_1).

Source	DF	Seq SS	Contribution	Adj MS	F-Value	P-Value
Linear	2	397.11	92.00%	198.555	74.79	<0.0001
A- Preparation method	1	30.20	7.00%	30.195	11.37	0.005
D- Chitosan conc	1	366.91	85.01%	366.914	138.20	<0.0001

a

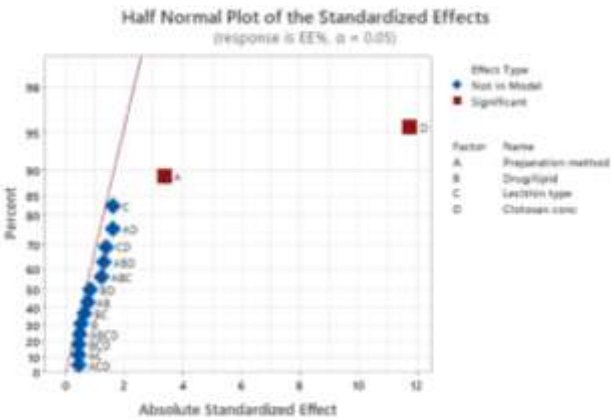

b

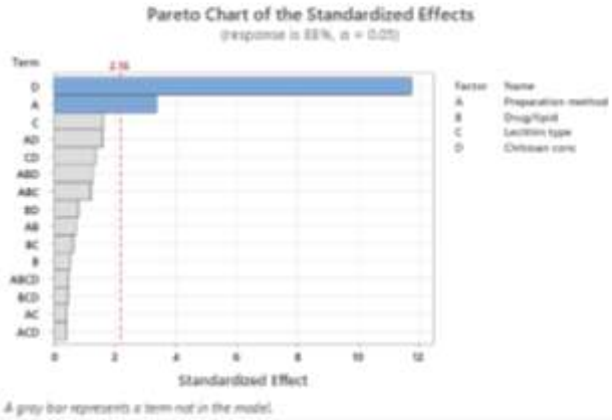

c

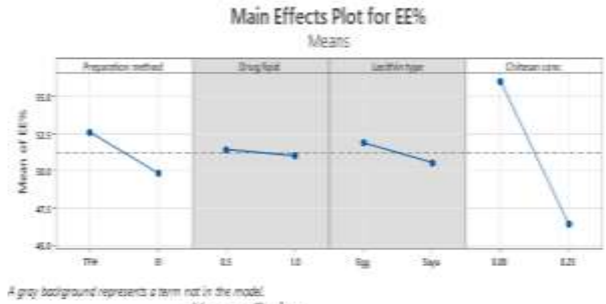

d

ISSN 1110-5089
ISSN (on-line) 2356_9786

e

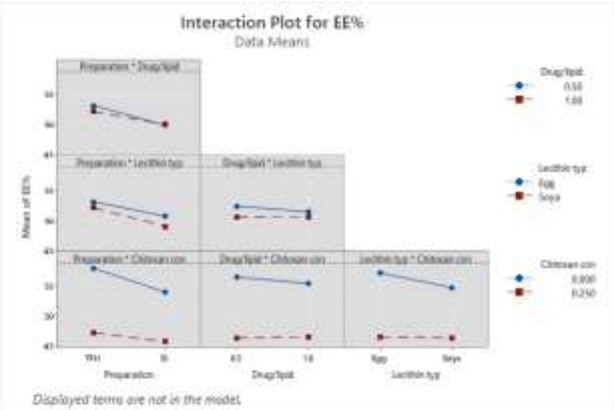

Figure 1: Half-normal probability plot (a) Pareto chart (b) for the factors and their interactions for EE%. Residuals versus runs plot (c). Main effects plot (d) and interaction plot (e) for EE%.

4.2. The effect of formulation variables on particle size and zeta potential

As displayed in Table 2, the particle size measurements of the prepared formulations ranged from 65.02 ± 1.02 nm (F12) to 670.90 ± 50.89 nm (F4). Meanwhile, the zeta potential was between -31.1 ± 1.54 for uncoated liposome (F9) and 46.9 ± 1.14 for chitosan-coated liposome (F16). Table 3 presents the significance of the proposed models for both particle size and zeta potential, as indicated by the high F-values of 65.38 and 386.84, respectively. Additionally, the coefficients of determination (R^2) were calculated to be 0.977 for particle size and 0.965 for zeta potential, confirming the excellent fit of these models. Moreover, in Figures 2c and 3c, it is evident that no significant outliers were present in the investigated results of particle size and zeta potential. After eight steps of selection, the model for particle size was developed by considering all the linear terms and two significant interactions, and the AICc was 191.19. The coded model equation for particle size = 215.0 - 57.8 A - 84.1 B - 143.5 C + 987.9 D - 577.7 AD + 150.6 BC. Whereas, the chitosan concentration was the only selected term after AICc minimization to 109.67. The chitosan concentration has impacted zeta potential with a contribution of 96.51% among all single factors and interactions. The coded equation presenting the model was Zeta potential = 20.49 + 244.0 D. The graphical representation in Figures 2d and 3d illustrates the impact of each factor on the particle size and zeta potential.

4.2.1. The effect of the liposome preparation method

The investigation of the single factor plots in Figure 2d showed that EI method yielded liposomes with significantly reduced particle size in comparison to TFH (P-value < 0.0001). That effect has contributed to 41.14 of the total effects presented by the suggested model with a relatively high F-value (165.08). It was observed that the particle size of the uncoated formulation formed of 1:1 drug to lipid with egg lecithin obtained through the EI method (F12) measured 65.2 ± 1.02 nm, while the formulation prepared using the TFI method (F2) had a particle size of 175.60 ± 15.15 nm. These results were concordant with previous reports that compared the effects of both methods on the particle size (30,31). Despite that, the preparation method did not exert any significant change on the zeta potential (P-value > 0.05).

4.2.2. The effect of drug/lipid ratio

In this study, altering the drug/lipid ratio had no statistically significant influence on the zeta potential and particle size of the liposomal vesicles. This suggests that the drug content does not significantly impact the surface charge or overall size of the vesicles, ensuring consistent and stable liposomal formulations for drug delivery.

4.2.3. The effect of lecithin type

This study revealed that there were no significant differences in particle charge when using either egg or soya lecithin for liposomes. However, a notable

Zagazig J. Pharm. Sci. Dec, 2023
Vol. 32, Issue 2, pp. 64-85
ISSN 1110-5089
ISSN (on-line) 2356_9786

impact on particle size was observed (P=0.014). Liposomes formulated with soya lecithin exhibited smaller particle sizes compared to those formulated with egg lecithin. The particle size of the uncoated formulation created with a 1:2 drug to lipid ratio using soya lecithin and obtained through the EI method (F1) was measured at 86.66 ± 2.70 nm. In contrast, the formulation containing egg lecithin (F15) exhibited a larger particle size of 138.10 ± 5.55 nm. Conversely, the coated formulations displayed a noticeable rise in particle size upon transitioning from soya lecithin to egg lecithin. This change resulted in particle sizes of 160.70 ± 13.76 nm for F16 and 325.00 ± 12.45 nm for F11. These findings are in line with previous research conducted by Yussof et al. in 2023 (32).

4.2.4. The effect of chitosan coating

The chitosan coating significantly influenced both the particle charge and size. The coating process increased particle size, and the charge was inverted to a positive one. Chitosan had a substantial impact on particle size, contributing 37% to the suggested model ($p<0.0001$). Additionally, chitosan was the sole contributor in the model explaining the effect on zeta potential ($p<0.0001$), which increased up to +46.9 for F16.

4.2.5. Two-way interactions

In order to examine the interaction between different factors and their impact on particle size, factorial plots were utilized. These plots incorporated all terms within the interaction plots, providing a visual representation of how the particle size varies when the levels of two factors are simultaneously altered. Based on the observations depicted in Figures 2e and 3e, it can be concluded that there was a high degree of parallelism between the two lines, indicating a lack of significant effects between the majority of interaction terms being studied. It was evident from the analysis that each individual factor had a distinct influence on the vesicle size. Out of the six potential interactions investigated, only two interactions were found to significantly impact the vesicle size. However, none of the interaction terms showed statistical significance in relation to the zeta potential. As seen in Figure 2e, the preparation method and chitosan coating showed an important interaction effect on the particle size. The particle size of liposomes was significantly reduced while using EI, while the vesicle was coated with 0.25% chitosan (P-value < 0.0001).

Table 6. Results of ANOVA statistical analysis of particle size (Y_2).

Source	DF	Seq SS	Contribution	Adj MS	F-Value	P-Value
Linear	4	536323	81.61%	134081	81.87	<0.0001
A-Preparation method	1	270338	41.14%	270338	165.08	<0.0001
B-Drug/lipid	1	7076	1.08%	7076	4.32	0.067
C-Lecithin type	1	14933	2.27%	14933	9.12	0.014
D-Chitosan conc	1	243977	37.12%	243977	148.98	<0.0001
Two-way Interactions	2	106126	16.15%	53063	32.40	<0.0001
AD-Preparation method*Chitosan conc	1	83440	12.70%	83440	50.95	<0.0001
BC-Drug/lipid*Lecithin type	1	22686	3.45%	22686	13.85	0.004

Table 7. Results of ANOVA statistical analysis of zeta potential (Y3).

Source	DF	Seq SS	Contribution	Adj MS	F-Value	P-Value
Linear	1	14884.0	96.51%	14884.0	386.84	<0.0001
D-Chitosan conc	1	14884.0	96.51%	14884.0	386.84	<0.0001

a

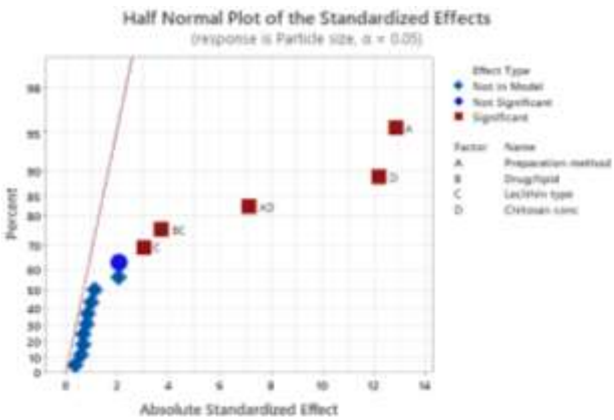

ISSN 1110-5089
ISSN (on-line) 2356_9786

b

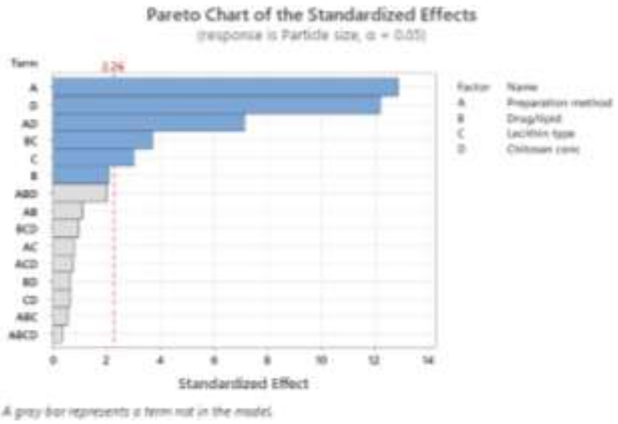

c

d

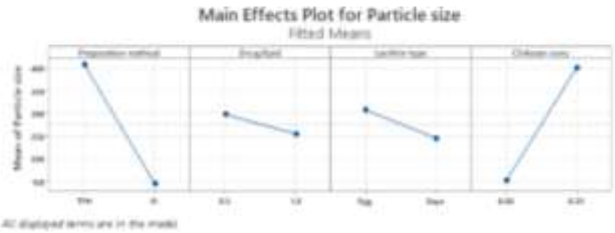

e

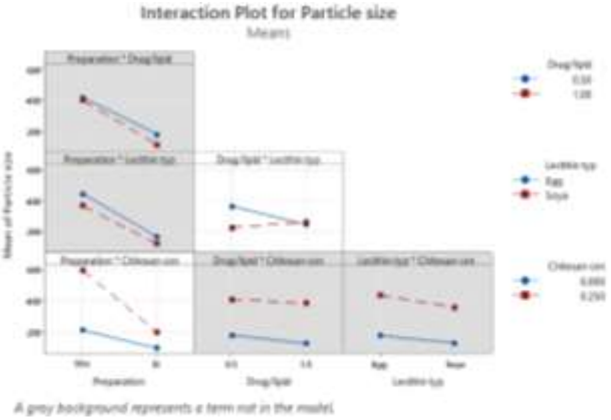

Figure 2: Half-normal probability plot (a) Pareto chart (b) for the factors and their interactions for particle size. Residuals versus runs plot (c). Main effects plot (d) and interaction plot (e) for particle size

a

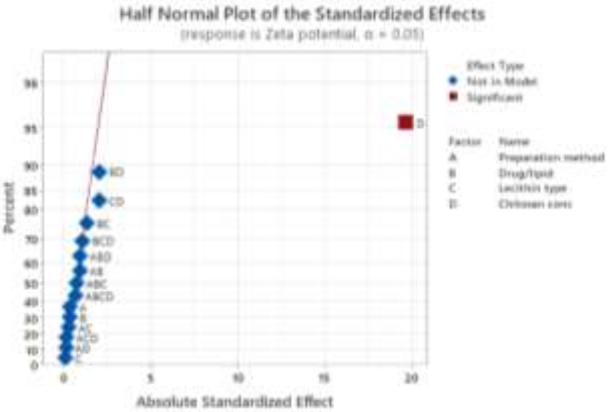

b

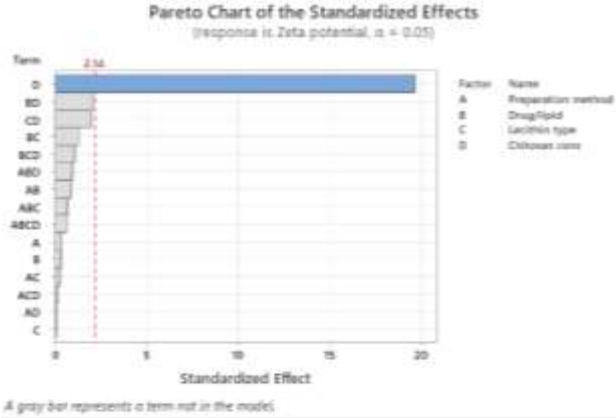

Zagazig J. Pharm. Sci. Dec, 2023
Vol. 32, Issue 2, pp. 64-85

ISSN 1110-5089
ISSN (on-line) 2356_9786

c

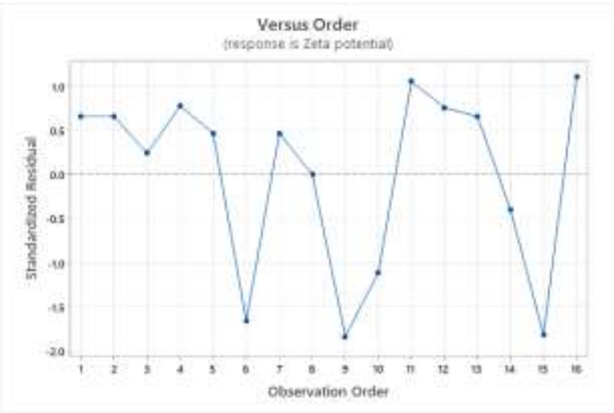

d

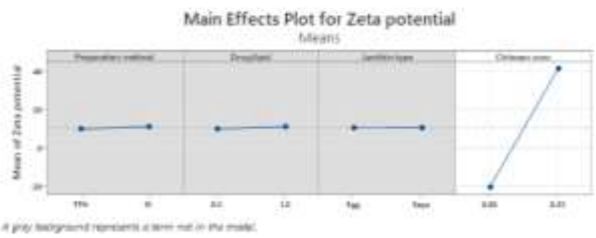

e

Figure 3: Half-normal probability plot (a) Pareto chart (b) for the factors and their interactions for zeta potential. Residuals versus runs plot (c). Main effects plot (d) and interaction plot (e) for zeta potential.

4.3. The effect of formulation variables on dissolution efficiency (DE%)

As shown in Table 2, the DE% of the prepared formulations ranged from 79.37 ± 2.54 (F1) to 90.69 ± 2.13% (F16) after 6 hours. As shown in Table 3, the model F-value of 203.24 implies the significance of the model with a coefficient of determination (R^2) = 0.980, indicating a good fit model. The *in vitro* release of granisetron from the liposomal and chitosan-coated liposomal dispersion in pH 7.4 is given in Figure 5. The drug was released in a biphasic manner from all formulations. A burst drug release was observed in the first 1 hr, in which the drug release reached and exceeded 50% in all formulations. This fast-release pattern was followed by a sustained release pattern until complete drug release was achieved in 6 hr for all formulations. The fast-release phenomenon was ascribed to the free granisetron adsorbed on the liposomal surface. This unentrapped granisetron finds an easier way to diffuse to the drug release interface and dissolve faster than the entrapped amount, which is slowly released. The coded model equation for DE% = 75.430 + 8.835 Drug/lipid + 58.03 Chitosan conc - 36.78 Drug/lipid*Chitosan conc.

4.3.1. Effect of preparation method and lecithin type

It can be concluded that both the preparation method either TFH or EI and the drug/lipid fraction exhibited a non-significant effect on the dissolution efficiency of granisetron (P-value > 0.05).

4.3.2. Effect of drug/lipid ratio

The study demonstrated a significant effect on DE % when the lipid content in liposomes was reduced, as indicated by the low p-value (<0.0001). Liposomes with a drug-to-liquid ratio of 1:2 exhibited slower drug release, particularly within the first hour. These results align with findings from Johnston et al. 2008, who observed similar effects of drug-to-lipid ratio on doxorubicin release behavior from liposomes (33). The slower release may imply a more stable formulation, which can be advantageous in various applications The drug dissolution efficiency (DE%) of the uncoated liposomal formulation, comprising a 1:1 drug to lipid ratio using soya lecithin and prepared through the EI

Zagazig J. Pharm. Sci. Dec, 2023
Vol. 32, Issue 2, pp. 64-85

ISSN 1110-5089
ISSN (on-line) 2356_9786

method (F13), was measured at 83.44 ± 2.55%. In contrast, the respective formulation (F1) with an elevated drug to lipid ratio exhibited a slightly lower DE% of 79.95 ± 2.54%.

4.3.3. The effect of chitosan coating

The presence of chitosan significantly impacted the dissolution of granisetron at pH 7.4, contributing to 83.91% of the effect. Consequently, the application of a chitosan coat to formulation F1, characterized by a DE% of 79.95 ± 2.54, led to an augmented release of granisetron, with F16 achieving a release of 90.69 ± 2.13%. This behavior can be explained by the competition between chitosan and granisetron for binding to the phospholipid, which was discussed previously (21). Chitosan's positive charges and affinity for the phospholipid surface lead to limited available binding sites, promoting the release of granisetron.

4.3.4. Two-way interaction

The analysis results reveal that, apart from a single significant interaction between drug-to-lipid ratio and chitosan coating (p<0.0001), none of the included interaction terms had a notable impact on the dissolution efficiency of granisetron. The supporting evidence provided by Figure 4e reinforces the significance of this particular interaction. The decision to incorporate these 2-way interaction terms in the model equation was guided by their contribution percentages (7.65%) and substantial F-value (47.59), indicating their meaningful influence on drug dissolution efficiency.

Table 8. Results of ANOVA statistical analysis of DE% (Y_4).

Source	DF	Seq SS	Contribution	Adj MS	F-Value	P-Value
Linear	2	249.681	90.42%	124.840	281.07	<0.0001
B-Drug/lipid	1	17.956	6.50%	17.956	40.43	<0.0001
D-Chitosan conc	1	231.725	83.91%	231.725	521.71	<0.0001
Two-way Interactions	1	21.137	7.65%	21.137	47.59	<0.0001
BD-Drug/lipid*Chitosan conc	1	21.137	7.65%	21.137	47.59	<0.0001

a

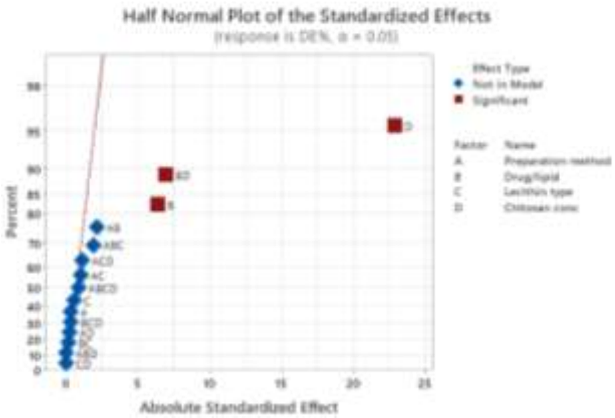

b

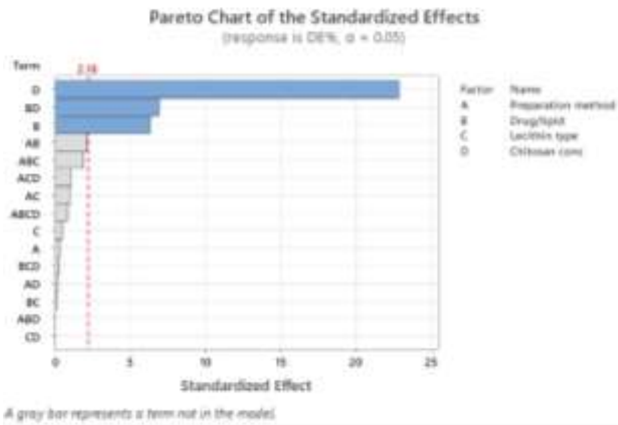

c

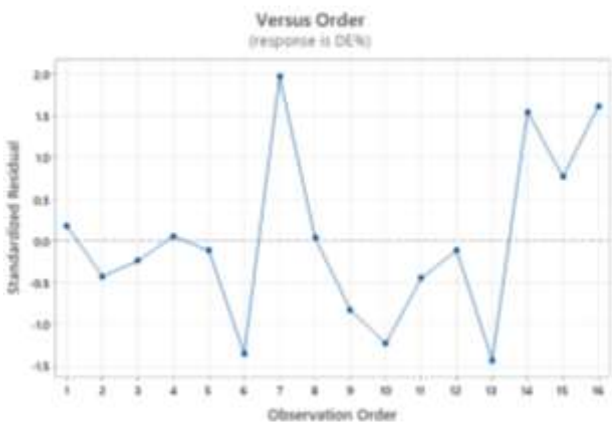

Zagazig J. Pharm. Sci. Dec, 2023
Vol. 32, Issue 2, pp. 64-85
ISSN 1110-5089
ISSN (on-line) 2356_9786

d

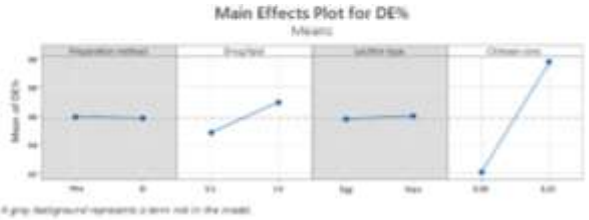

e

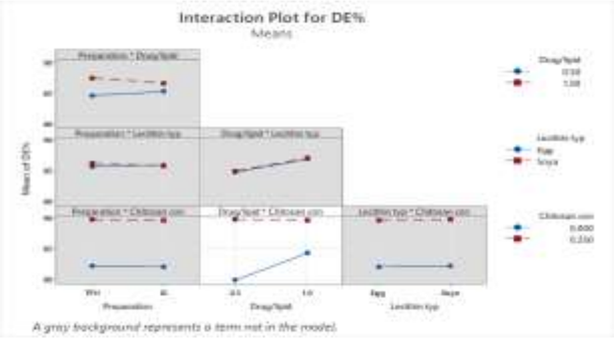

Figure 4: Half-normal probability plot (a) Pareto chart (b) for the factors and their interactions for DE%. Residuals versus runs plot (c). Main effects plot (d) and interaction plot (e) for DE%.

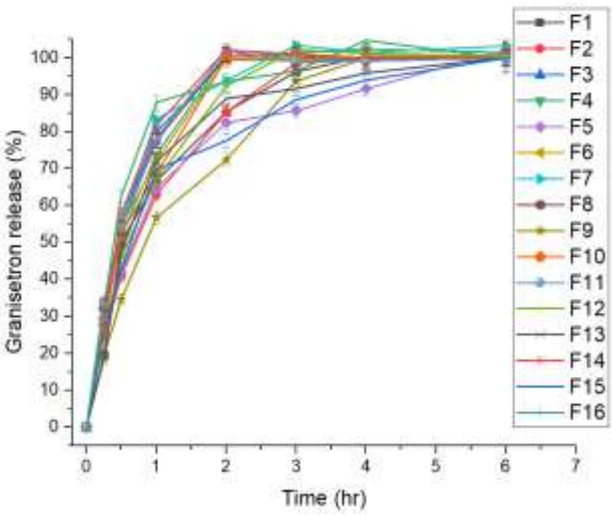

Figure (5): Release of granisetron from coated and uncoated liposomal formulations in pH 7.4.

4.4. Optimization of granisetron-loaded liposomal formulation.

The optimized granisetron-loaded liposomal formulation was prepared as suggested by optimization findings and characterized as follows:

4.4.1. Formulation variables EE%, Particle size, Zeta potential, and DE%

The optimization followed the targets presented in Table 1, which aimed to attain specific levels of the studied variables. Based on previously published criteria, the required criteria relied on targeting the particle size of liposomal vesicles to around 120 nm, and the zeta potential was set to +35 Ve. Meanwhile, other responses (EE%, and DE%) were set at the maximum possible outcomes. Concerning the highest desirability value (0.635), the formulation containing Soya lecithin at drug to lipid ratio of 1:1, prepared by ether injection method and coated with 0.143% w/w of chitosan, was chosen after optimization. As predicted by Minitab, the values for EE%, particle size, zeta potential, and DE% were 49.11%, 127.33 nm, 14.65 Ve, and 87.32%, respectively. After the optimized formulation was prepared and characterized accordingly, the experimental values for the previously stated responses were 47.29% ± 2.23, 137.25 ± 5.72 nm, 17.14 ± 1.71 Ve and 86.82% ± 7.68, respectively (Figure 6). The observed and predicted values demonstrated a high level of agreement. This suggests that the optimization tools utilized in the study performed effectively, accurately predicting the outcomes.

Zagazig J. Pharm. Sci. Dec, 2023
Vol. 32, Issue 2, pp. 64-85
ISSN 1110-5089
ISSN (on-line) 2356_9786

a

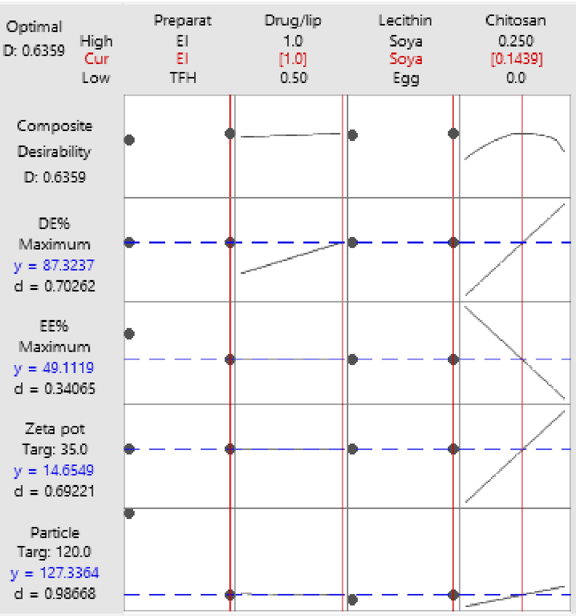

b

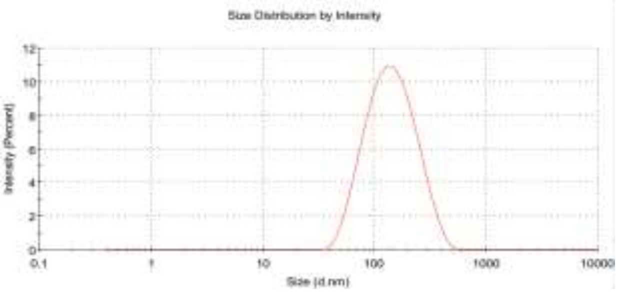

c

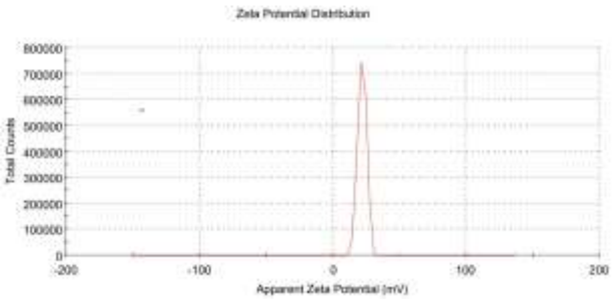

d

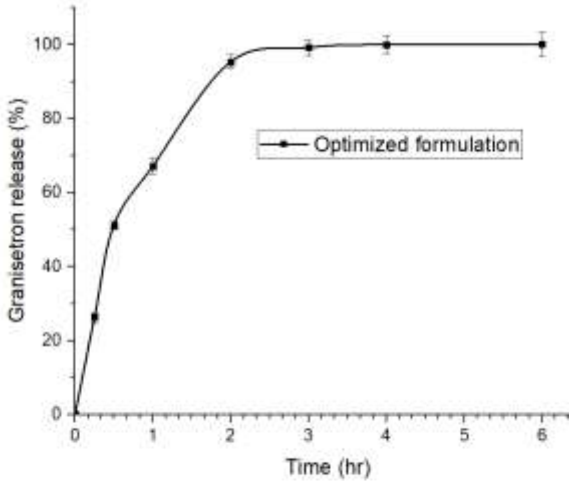

e

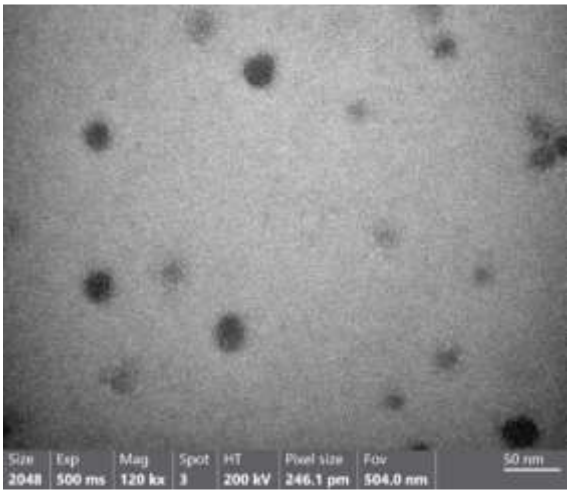

Figure 6: (a) Desirability profile for multiple response optimization. (b) Particle size, (c) zeta potential, (d) dissolution efficiency percentage and (e) TEM image of the optimized granisetron-loaded liposomes.

4.4.2.Transmission electron microscopy (TEM)

The optimized liposomal preparation was imagined via a Talos™ F200i TEM. Figure 6e clearly proves the nanovesicles as spherical particles devoid of aggregates, implying their uniform size. The particle size values obtained through the DLS technique exhibited a slight discrepancy, with slightly higher measurements than those obtained through TEM analysis. The variation in particle size measurements between the DLS technique and TEM analysis can be

Zagazig J. Pharm. Sci. Dec, 2023
Vol. 32, Issue 2, pp. 64-85
ISSN 1110-5089
ISSN (on-line) 2356_9786

attributed to the differences in measurement conditions, with TEM analyzing dried liposomes and DLS accounting for the presence of water molecules surrounding the particles (22).

4.4.3. The investigation of chemical interaction

The interaction between granisetron and the ingredients of the coated liposomes was shown in the FTIR spectra (Figure 7a). The FTIR study conducted on granisetron revealed several major peaks in its spectrum. These peaks were observed at specific wavenumbers, providing important insights into the molecular composition and functional groups present within granisetron. At 3232 cm^{-1}, a significant peak corresponding to the NH was noted. Other notable peaks include those at 2946 cm^{-1}, indicating C-H stretching. The presence of a peak at 1645 cm^{-1} reveals the stretching of the C=O bond in the CONH group, while the peak at 1610 cm^{-1} signifies the stretching of the C=N bond, further characterizing the granisetron molecule. Moreover, peaks at 1546, 1474, and 1435 cm^{-1} correspond to the stretching of C=C bonds within aromatic rings, providing evidence of conjugated systems in granisetron. Lastly, a peak at 1413 cm^{-1} indicates C-N stretching, which is further evidence of the presence of amine groups within the molecule. These findings were in accordance with Sahoo et al. 2016 (34).

On the other hand, cholesterol showed an absorption peak observed at 3423 cm^{-1} indicating O-H stretching vibrations. The absorptions at 2930 and 2866 cm^{-1} can be attributed to C-H stretching vibrations, indicating the existence of hydrocarbon chains. Furthermore, absorptions at 1464 and 1376 cm^{-1} represent C-H bending vibrations, indicating the flexibility of the molecular structure and the existence of multiple carbon-hydrogen bonds. Additionally, absorptions at 1235, 1131, 1054, and 1022 cm^{-1} suggest C-O stretching vibrations of esters (35).

Moreover, the FTIR spectrum of soy lecithin exhibited distinct peaks at 3374 and 1745 cm^{-1}, corresponding to the stretching frequencies of O-H and C=O bonds, respectively, as reported by Siyal et al. 2020 (36). Additionally, stretching vibrational peaks observed at 1170 and 1062 cm^{-1} can be attributed to C-O and C-C bonds within the soya lecithin molecule (as shown in Figure 7a, green line). In the FTIR spectrum of chitosan, distinct peaks were observed at 3353 cm^{-1}, corresponding to the stretching vibrations of the O-H group and asymmetrical stretching of the N-H bond, respectively. These peaks clearly indicate the presence of hydroxyl (O-H) and amide groups in chitosan (37,38). Peaks at 1652 and 1581 cm^{-1} are assigned to bending the -NH (amine) group. Additional small peaks were observed at 1374 cm^{-1}, indicating C-N amine stretching, and the intensely broad peak at 1023 cm^{-1}, representing the stretching vibrations of primary alcohols within the C-O and C-N groups.

The physical mixture has retained most of the characteristic peaks of granisetron and other excipients. However, the optimized chitosan-coated liposomes showed a slightly different pattern from the physical mixture, specifically at the position of 1085, which is a characteristic feature of chitosan (C-N amine stretching). This implies that chitosan was successfully bound to the surface of the liposomes. Additionally, other peaks at 1649 cm^{-1} might be explained by the presence of unentrapped granisetron.

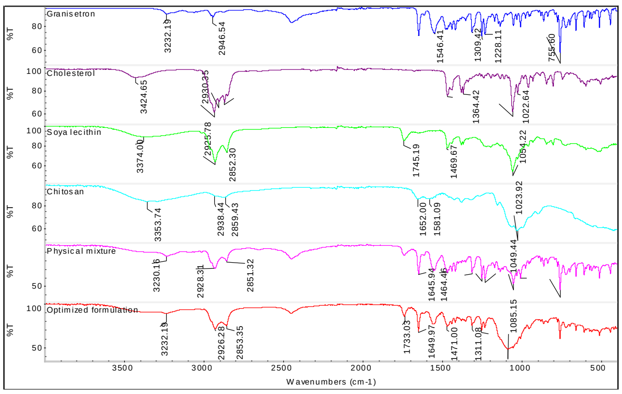

ISSN 1110-5089
ISSN (on-line) 2356_9786

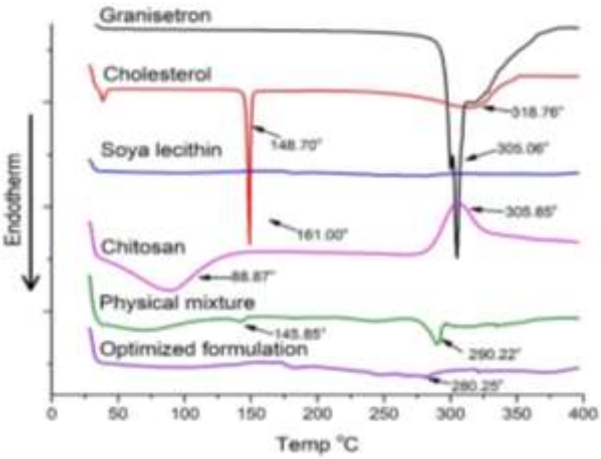

Figure 7. (a) FTIR spectra of liposome ingredients and the optimized liposomal formulation. (b) DSC thermograms of liposome ingredients and the optimized liposomal formulation.

4.4.4. Differential scanning calorimetry

Figure 7b displays the DSC thermograms for granisetron HCl and cholesterol. The determined glass transition temperature (Tg) values were observed at 305.05 ºC for granisetron and 148.7 ºC for the polymer, which aligns with previously reported values in the literature (39,40). Notably, the characteristic sharp exothermic peak observed at 305.85 °C in Figure 7b aligns with the DSC thermogram reported previously in the literature (41). Soya lecithin did not exhibit any melting peaks as seen in the thermogram, which is consistent with results reported by Dubey and Shirat (42). The physical mixture retained the peak corresponding to granisetron with a minor shifting to 290º, and cholesterol content was slightly obvious at 145.85º. The optimized formulation showed no significantly observed peaks at 305 ºC. Meanwhile, a minor peak at 280 ºC was observed, which implies that granisetron was successfully entrapped into the liposome.

4.5. Characterization of the liposomal vesicles-loaded hydrogel:

4.5.1. pH, drug content and viscosity of the formulated hydrogel:

The hydrogel was subjected to characterization tests to ensure the pertinence of the hydrogel base for further applications. The gel formulations' pH was 6.54 ± 0.13 and 7.62 ± 0.27 for G1 and G2, respectively, as reported in Table 8. The pH of prepared formulations exhibited similarity to the skin pH to avoid irritation, redness, dryness, and inflammation (42). Moreover, the drug content of the hydrogel ranged from 97.14 ± 1.95 to 101.87 ± 2.18 % for G3 and G2, respectively. These results imply that granisetron-loaded liposomal vesicles were homogeneously distributed in the hydrogel.

The viscosity of the gel matrix plays a crucial role in controlling the drug release rate (43). The presence of the liposome led to a slight increase in the viscosity of the prepared hydrogel formulations. The viscosity of the prepared hydrogels ranged from 8633.33 ± 124.72 to 9500 ± 81.64 centipoise for G2 and G3, respectively. Moreover, the viscosity was increased in the case of Na CMC (2%, w/v), while HPMC-E4M exhibited lower viscosities at a higher concentration 3% (w/v).

Table 9. The composition and characterization properties of granisetron and liposome-embedded hydrogel.

Code	Drug form	Gel base	pH	Drug content (%)	Viscosity (Centipoise)
G1	Granisetron	HPMC	6.54 ± 0.13	98.41 ± 1.74	9266.66 ± 205.48
G2	Granisetron	Na CMC	7.62 ± 0.27	101.87 ± 2.18	8633.33 ± 124.72
G3	Liposomes	HPMC	6.67 ± 0.21	97.14 ± 1.95	9500 ± 81.64
G4	Liposomes	Na CMC	7.43 ± 0.18	99.47 ± 1.26	8800 ± 294.39

4.5.2. Drug release from liposome-embedded hydrogels:

The drug release percentages from liposomal hydrogel are shown in Figure 8a. It was observed that the release from the hydrogel base is correlated with the gel base viscosity. The viscosity of HPMC was lower than that of Na CMC, therefore the HPMC base exhibited a weaker effect on impeding the granisetron release. The hydrogel networks are believed to exert a significant effect on the viscosity through the van-der Waals forces. These forces are also increased by the gel polymer concentration leading to augmented viscosity, which

Zagazig J. Pharm. Sci. Dec, 2023 ISSN 1110-5089
Vol. 32, Issue 2, pp. 64-85 ISSN (on-line) 2356_9786

consequently affects the drug release. The drug release of granisetron was observed to continue for up to 6 hrs reaching about 100%. Meanwhile, in the case of the Na CMC base, the release was slightly slower than that from HPMC. Therefore, the HPMC gel base was chosen for further *ex-vivo* skin permeation testing.

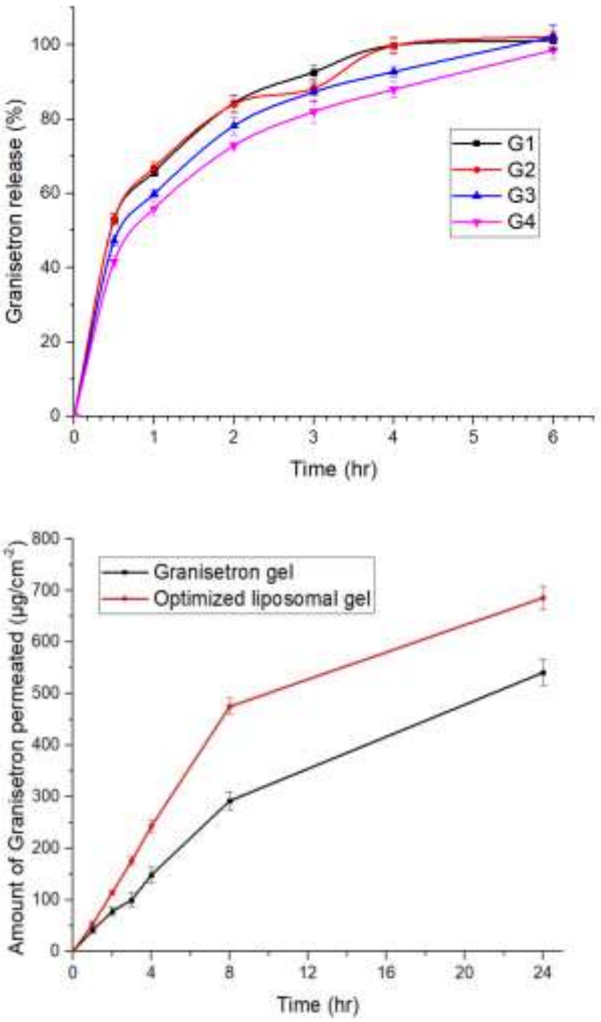

Figure 8. (a) In-vitro drug release from the gel bases. (b) Ex vivo skin permeation study of the optimized liposomal gel versus granisetron gel.

4.5.3. Ex vivo skin permeation of the liposomal hydrogel:

Skin permeation studies are crucial for assessing the granisetron release behavior from prepared hydrogel formulations (G1 and G3). The results for granisetron permeated through rabbit ear skin are shown in Figure (8b). Cumulative granisetron permeated in 24 hr , and steady-state fluxes (Jss) were calculated and used to evaluate the effect of granisetron loading into liposomal vesicles on the permeation through rabbit ear skin.

The selected optimized liposomal gel formulation (G3) exhibited a higher amount of granisetron permeated through the skin (686.22 ± 48.29 µg/cm^2) following 24 hr when compared to those of control gel formulation (G1) (541.22 ± 34.82 µg/cm^2 after 24 hr). The flux (Jss) of granisetron-loaded liposomal formulation (G3) through the rabbit ear was significantly increased ($p < 0.05$) in comparison with the granisetron gel (G1). The mean flux of G3 was 27.73 µg.cm^{-2}.hr^{-1}, which was increased by about 25% compared to G1 (22.03 µg.cm^{-2}.hr^{-1}). The enhanced permeation of granisetron released from liposomes, particularly in the presence of tween 80 as a penetration enhancer, is due to synergistic and favorable interactions between liposomes and skin components (46).

Conclusion:

The development and evaluation of chitosan-coated liposomal vesicles as a transdermal drug delivery system for granisetron hydrochloride showed promising potential. Optimization of the formulation led to favorable characteristics such as a targeted particle size and zeta potential. The liposomal formulations demonstrated superior drug delivery capabilities compared to conventional gel formulations. These liposomal-loaded formulations exhibited enhanced transdermal delivery of granisetron, indicating their potential for improving therapeutic outcomes in chemotherapy-induced nausea and vomiting. Further research and clinical studies are needed to validate the effectiveness and safety of these liposomal systems for broader applications.

Acknowledgement:

The authors are thankful to Mohamed Salah Attia (Department of Pharmaceutics, Faculty of Pharmacy, Zagazig University) for his assistance in the data analysis of this article.

REFERENCES

1. Salihah N, Mazlan N, Lua PL. Chemotherapy-induced nausea and vomiting: exploring patients' subjective experience. J Multidiscip Healthc. 2016;145–51.

2. Bender CM, McDaniel RW, Murphy-Ende K, Pickett M, Rittenberg CN, Rogers MP, et al. Chemotherapy-induced nausea and vomiting. Clin J Oncol Nurs. 2002;6(2).

3. Kovac AL. Postoperative and postdischarge nausea and vomiting after ambulatory surgery: An update. Curr Anesthesiol Rep. 2014;4:316–25.

4. Plosker GL, Goa KL. Granisetron: a review of its pharmacological properties and therapeutic use as an antiemetic. Drugs. 1991;42:805–24.

5. Attia MS, Hasan AA, Ghazy FES, Gomaa E. Solid Dispersion as a Technical Solution to Boost the Dissolution Rate and Bioavailability of Poorly Water-Soluble Drugs. Indian J Pharm Educ Res. 55(3):13.

6. Ahmed S, El-Setouhy DA, Badawi AAEL, El-Nabarawi MA. Provesicular granisetron hydrochloride buccal formulations: In vitro evaluation and preliminary investigation of in vivo performance. Eur J Pharm Sci. 2014;60:10–23.

7. Çağdaş M, Sezer AD, Bucak S. Liposomes as potential drug carrier systems for drug delivery. Appl Nanotechnol Drug Deliv. 2014;1:1–50.

8. Alavi M, Karimi N, Safaei M. Application of various types of liposomes in drug delivery systems. Adv Pharm Bull. 2017;7(1):3.

9. Ammar HO, Mohamed MI, Tadros MI, Fouly AA. Transdermal delivery of ondansetron hydrochloride via bilosomal systems: in vitro, ex vivo, and in vivo characterization studies. AAPS PharmSciTech. 2018;19:2276–87.

10. Escobar-Chávez JJ, Díaz-Torres R, Rodriguez-Cruz I, Domínguez-Delgado C, Morales R, Ángeles-Anguiano E, et al. Nanocarriers for transdermal drug delivery. skin. 2012;19:22.

11. Bhowmik D, Pusupoleti KR, Duraivel S, Kumar KS. Recent approaches in transdermal drug delivery system. Pharma Innov. 2013;2(3, Part A):99.

12. Patil BA. Formulation and development of industry feasible proniosomal transdermal drug delivery system of granisetron hydrochloride. Asian J Pharm AJP. 2015;113–9.

13. Aggarwal G, Kumar V, Chaudhary H. Design, Optimization and Characterization of Granisetron HCl Loaded Nano-gel for Transdermal Delivery. Pharm Nanotechnol. 2017;5(4):317–28.

14. Lee MK. Liposomes for enhanced bioavailability of water-insoluble drugs: in vivo evidence and recent approaches. Pharmaceutics. 2020;12(3):264.

15. Shah D, Londhe V. Optimization and characterization of levamisole-loaded chitosan nanoparticles by ionic gelation method using 23 factorial design by Minitab® 15. Ther Deliv. 2011;2(2):171–9.

16. Moghimipour E, Handali S. Utilization of thin film method for preparation of celecoxib loaded liposomes. Adv Pharm Bull. 2012;2(1):93.

17. Nwobodo NN, Adamude F, Dingwoke E, Ubhenin A. Formulation and evaluation of elastic liposomes of decitabine prepared by rotary evaporation method. Univers J Pharm Res. 2019;4(3):1–5.

ISSN 1110-5089
ISSN (on-line) 2356_9786

18. Kumar A, Badde S, Kamble R, Pokharkar VB. Development and characterization of liposomal drug delivery system for nimesulide. Int J Pharm Pharm Sci. 2010;2(4):87–9.

19. Kanda H, Katsube T, Wahyudiono, Goto M. Preparation of liposomes from soy lecithin using liquefied dimethyl ether. Foods. 2021;10(8):1789.

20. Zaru M, Manca ML, Fadda AM, Antimisiaris SG. Chitosan-coated liposomes for delivery to lungs by nebulisation. Colloids Surf B Biointerfaces. 2009;71(1):88–95.

21. Guo J xin, Ping Q neng, Jiang G, Huang L, Tong Y. Chitosan-coated liposomes: characterization and interaction with leuprolide. Int J Pharm. 2003;260(2):167–73.

22. Attia MS, Radwan MF, Ibrahim TS, Ibrahim TM. Development of Carvedilol-Loaded Albumin-Based Nanoparticles with Factorial Design to Optimize In Vitro and In Vivo Performance. Pharmaceutics. 2023;15(5):1425.

23. Shaker S, Gardouh AR, Ghorab MM. Factors affecting liposomes particle size prepared by ethanol injection method. Res Pharm Sci. 2017;12(5):346.

24. Gomaa E, Attia MS, Ghazy FES, Hassan AE, Hasan AA. Pump-free electrospraying: A novel approach for fabricating Soluplus®-based solid dispersion nanoparticles. J Drug Deliv Sci Technol. 2022;67:103027.

25. Ibrahim MM, Hafez SA, Mahdy MM. Organogels, hydrogels and bigels as transdermal delivery systems for diltiazem hydrochloride. Asian J Pharm Sci. 2013;8(1):48–57.

26. Nasr M, Younes H, Abdel-Rashid RS. Formulation and evaluation of cubosomes containing colchicine for transdermal delivery. Drug Deliv Transl Res. 2020;10:1302–13.

27. Zulfakar MH, Abdelouahab N, Heard CM. Enhanced topical delivery and ex vivo anti-inflammatory activity from a betamethasone dipropionate formulation containing fish oil. Inflamm Res. 2010;59:23–30.

28. Hussain A, Khan GM, Shah SU, Shah KU, Rahim N, Wahab A, et al. Development of a novel ketoprofen transdermal patch: Effect of almond oil as penetration enhancers on in-vitro and ex-vivo penetration of ketoprofen through rabbit skin. Pak J Pharm Sci. 2012;25(1).

29. BUKKA R, HN C. HIGH-PERFORMANCE LIQUID CHROMATOGRAPHIC ESTIMATION METHOD FOR TRANSDERMAL DIFFUSION STUDY OF GRANISETRON. Asian J Pharm Clin Res. 2021;14(4):105–8.

30. Alyami H, Abdelaziz K, Dahmash EZ, Iyire A. Nonionic surfactant vesicles (niosomes) for ocular drug delivery: Development, evaluation and toxicological profiling. J Drug Deliv Sci Technol. 2020;60:102069.

31. Jadon PS, Gajbhiye V, Jadon RS, Gajbhiye KR, Ganesh N. Enhanced oral bioavailability of griseofulvin via niosomes. AAPS Pharmscitech. 2009;10:1186–92.

32. Yussof NS, Ping TC, Boon TT, Utra U, Ramli ME. Influence of Soy Lecithin and Sodium Caseinate on The Stability and in vitro Bioaccessibility of Lycopene Nanodispersion. Food Technol Biotechnol. 2023;61(1):39–50.

33. Johnston MJ, Edwards K, Karlsson Gör, Cullis PR. Influence of drug-to-lipid ratio on drug release properties and liposome integrity in liposomal doxorubicin formulations. J Liposome Res. 2008;18(2):145–57.

ISSN 1110-5089
ISSN (on-line) 2356_9786

34. Sahoo CK, Sahoo NK, Sahu M, Sarangi DK. Formulation and Evaluation of Orodispersible Tablets of Granisetron Hydrochloride Using Agar as Natural Super disintegrants. Pharm Methods. 2016;7(1).

35. Vyas PM, Joshi M. Surface micro topographical and dielectric studies of cholesterol crystals. In Trans Tech Publ; 2013. p. 289–96.

36. Siyal FJ, Memon Z, Siddiqui RA, Aslam Z, Nisar U, Imad R, et al. Eugenol and liposome-based nanocarriers loaded with eugenol protect against anxiolytic disorder via down regulation of neurokinin-1 receptors in mice. Pak J Pharm Sci. 2020;33.

37. Agarwal M, Agarwal MK, Shrivastav N, Pandey S, Das R, Gaur P. Preparation of chitosan nanoparticles and their in-vitro characterization. Int J Life-Sci Sci Res. 2018;4(2):1713–20.

38. Lustriane C, Dwivany FM, Suendo V, Reza M. Effect of chitosan and chitosan-nanoparticles on post harvest quality of banana fruits. J Plant Biotechnol. 2018;45(1):36–44.

39. Jin Y, Wen J, Garg S, Liu D, Zhou Y, Teng L, et al. Development of a novel niosomal system for oral delivery of Ginkgo biloba extract. Int J Nanomedicine. 2013;421–30.

40. Yapar EA, Baykara T. Thermal analysis on phase sensitive granisetron in situ forming implants. J Appl Pharm Sci. 2014;4(7):010–3.

41. Saber-Samandari S, Yilmaz O, Yilmaz E. Photoinduced graft copolymerization onto chitosan under heterogeneous conditions. J Macromol Sci Part A. 2012;49(7):591–8.

42. Dubey M, Shirsat MK. Formulation And Evaluation Of Phytosome Tablet Of Plant Mangifera Indica. 2020;

43. Parashar P, Mazhar I, Kanoujia J, Yadav A, Kumar P, Saraf SA, et al. Appraisal of anti-gout potential of colchicine-loaded chitosan nanoparticle gel in uric acid-induced gout animal model. Arch Physiol Biochem. 2019;1–11.

44. El-Masry SM, Helmy SA. Hydrogel-based matrices for controlled drug delivery of etamsylate: Prediction of in-vivo plasma profiles. Saudi Pharm J. 2020;28(12):1704–18.

45. Sevinç-Özakar R, Seyret E, Özakar E, Adıgüzel MC. Nanoemulsion-Based Hydrogels and Organogels Containing Propolis and Dexpanthenol: Preparation, Characterization, and Comparative Evaluation of Stability, Antimicrobial, and Cytotoxic Properties. Gels. 2022;8(9):578.

46. Sahu K, Kaurav M, Pandey RS. Protease loaded permeation enhancer liposomes for treatment of skin fibrosis arisen from second degree burn. Biomed Pharmacother. 2017;94:747–57.

Zagazig J. Pharm. Sci. Dec, 2023 ISSN 1110-5089
Vol. 32, Issue 2, pp. 64-85 ISSN (on-line) 2356_9786

تحسين التوصيل عبر الجلد لعقار الجرانيسيترون عبر حويصلات دهنية مغلفة بالكيتوزان باستخدام 2^4 تصميمًا عامليًا كاملًا

ماجد عبدالله الشنواني ، عزة حسن ، سمير سيد أبو زيد ، شرين احمد صبري
.قسم الصيدلانيات ، كلية الصيدلة ، جامعة الزقازيق ، الزقازيق 44519 ، مصر

ملخص البحث

ركزت الدراسة الحالية على تطوير وتقييم الحويصلات الدهنية المغلفة بالشيتوزان كنظام لتوصيل الأدوية عبر الجلد لهيدروكلوريدجرانيسترون ، وهو دواء فعال مضاد للقيءيستخدم في الغثيان والقيء الناجم عن العلاج الكيميائي برنامج Minitab 21.4 تم استخدامه لتحسين أنظمة توصيل الجرانيسترون من خلال تصميم عاملي كامل مكون من 4 عوامل ومستويين. ركزت الدراسة المقترحة على عوامل الصياغة الرئيسية: طريقة التحضير ونسبة الدواء/الدهون، ونوع الليسيثين، وغلاف الشيتوزان، وتأثيرها على الاستجابات المقترح دراستها. قد ساعد هذا النهج في تحديد العوامل ذات الأهمية العالية في معادلة النموذج، مما عزز الفهم لتحسين صياغة الجرانيسيترون .تم إجراء دراسات الخصائص الفيزيائية والكيميائية ، معدل إنطلاق الدواء ، الحرائك الدوائية ، ودراسات نفاذ الجلد خارج الجسم الحي لتقييم التركيبات الشحمية. أشارت النتائج إلى أن التركيبات المحملة بالجسيمات الشحمية لديها القدرة على تعزيز التوصيل عبر الجلد للجرانيسترون مقارنة بتركيبات الهلام التقليدية. أكدت هذه النتائج على القدرات الفائقة لإيصال الأدوية للأنظمة الشحمية وقدرتها على تحسين النتائج العلاجية في التطبيق المستهدف. تهدف عملية التحسين إلى تحقيق أهداف محددة ، بما في ذلك حجم جسيم يبلغ حوالي 120 نانومتر وإمكانات زيتا تبلغ +35 فولت. أظهرت الصيغة المثلى المختارة قيمًا مواتية ، بكفاءة تغليف تبلغ 47.29٪ ، وحجم جسيم يبلغ 137.25 نانومتر ، وإمكانات زيتا 17.14 فولت ، وكفاءة إذابة 86.82٪. علاوة على ذلك ، أظهرت تركيبة الجل الدهني المحسن زيادة بنسبة 25 ٪ في التدفق (27.73 µg.cm-2.hr-1) مقارنة بالجيل الخام المحمّل بالدواء ((22.03 µg.cm-2.hr-1)) لتخلل جرانيسترون عبر الجلد.

الكلمات الدالة:

جرانيسيترون؛ الجسيمات الشحمية؛ توصيل عبر الجلد؛ الدهون الفسفورية؛ الشيتوزان؛ حجم الجسيمات؛ إمكانات زيتا ؛كفاءة الذوبان